Supplementary data

Title: RNA-seq-based miRNA signature as an independent predictor of relapse in pediatric B-cell acute lymphoblastic leukemia

Authors: Hirohito Kubota, Hiroo Ueno, Keiji Tasaka, Tomoya Isobe, Satoshi Saida, Itaru Kato, Katsutsugu Umeda, Mitsuteru Hiwatari, Daiichiro Hasegawa, Toshihiko Imamura, Nobuyuki Kakiuchi, Yasuhito Nannya, Seishi Ogawa, Hidefumi Hiramatsu, Junko Takita

Supplementary Methods

Survival analysis

Overall survival (OS) was calculated from the date of diagnosis to the date of death from any cause, and shorter event-free survival (EFS) was calculated from the date of diagnosis until the date of the first event (failure to achieve remission, relapse, secondary malignancy, or death by any cause) or the date of the last follow-up. The Kaplan–Meier method was used to estimate OS, EFS and their associated 95% confidence intervals (CIs), and the log-rank test was used to assess differences between the groups. Analyses were performed using the R package survival v3.2.13. The EFS was also evaluated using the Cox proportional-hazards model. The model included age, white blood cell count, MRD status at day 29, and miRNA cluster as covariates. P values of less than 0.05 were considered statistically significant. The R package survivalROC v1.0.3.1 was used to plot and calculate the area under the curve (AUC) of the time-dependent receiver operating characteristic (ROC) curve to evaluate the predictive power of prognostic model and miRNA expression.

miRNA signature training and validation

To extract a core subset of miRNAs from among the 219 most highly expressed (RPM > 25) miRNAs in the TARGET ALL cohort that best explained the miR-low cluster (MLC) signature in the discovery cohort, a linear regression technique based on the Lasso algorithm was used (as implemented in the glmnet v4.1.2 R package) while still enabling leave-one-out cross-validation to fit a Cox regression model.[1] The MLC score was calculated for each patient as a linear combination of the z-score-normalized expression (reads per million; RPM), using the mean and standard deviations from the training data (the TARGET ALL cohort) for the 19 miRNAs, weighted by regression coefficients estimated from the training data, as follows: MLC score = (miR-100-5p × 0.123) + (miR-1304-3p × 0.0116) + (miR-130b-5p × 0.0592) + (miR-146b-5p × −0.313)

+ (miR-181c-5p × -0.0303) + (miR-186-5p × -0.00347) + (miR-18a-3p × 0.119) + (miR-196b-5p × 0.104) + (miR-20b-5p × −0.0169) + (miR-28-5p × −0.0222) + (miR-324-5p × -0.108) + (miR-326 × −0.492) + (miR-361-5p × -0.0511) + (miR-4448 × 0.0496) + (miR-455-3p × 0.0556) + (miR-486-3p × 0.165) + (miR-582-3p × 0.054) + (miR-92a-1-5p x 0.00299) + (miR-92b-3p x 0.188) - 1.117. In the test cohort (the Japanese cohort), a group with a score in the highest tertile of the population was defined as having a high MLC score.

Copy number analysis based on SNP array data

Of the 111 cases in the TARGET ALL cohort, 105 had available single nucleotide polymorphism (SNP) array data (Affymetrix SNP Array 6.0). Raw copy number segmentation results from Affymetrix Genomewide SNP6 arrays were downloaded from (https://target-data.nci.nih.gov/Public/ALL/copy_number_array/Phase2/L3/). The GISTIC 2.0 method was used to identify significant copy number variations. G-scores were plotted along each chromosome using a 99% CI at a false discovery threshold of 5%. Copy number variants arising from immunoglobulin/T cell receptor gene rearrangements were excluded. *IKZF1*^{plus} was defined as *IKZF1* deletions co-occurring with deletions in *CDKN2A*, *CDKN2B*, *PAX5*, or *PAR1* in the absence of *ERG* deletion.[2]

DNA methylation analysis

Of the 111 cases in the TARGET ALL cohort, 53 had available DNA methylation data (HpaII tiny fragment Enrichment by Ligation-mediated PCR (HELP) Assay with Roche NimbleGen). DNA methylation was quantified using the median normalized log2 ratio of the HpaII to MspI signal intensity from the HELP Assay.

Whole exome sequencing (WES) and mutation calling

WES libraries were prepared using the Lotus DNA Library Prep Kit (IDT) and the xGen

Exome Research Panel (IDT), followed by sequencing of enriched exon fragments on an MGI DNBSEQ platform using a 150 bp paired-end read protocol. Candidate somatic mutations were identified using the Genomon pipeline v2.6.2. Variant calling of the WES data was conducted as follows: candidate mutations showing (1) a Fisher's exact test *P*-value of ≤ 0.1, (2) an Empirical Bayesian Mutation Calling *P*-value ≤ 0.001, and (3) a variant allele frequency in tumor samples > 5% were selected. These variants were further filtered by excluding (1) synonymous single nucleotide variants (SNVs), (2) SNVs in genes whose structures were not correctly annotated, and (3) SNVs listed as polymorphisms in the ExAc, ToMMO, tommo35K, 1000 Genomes Project, ESP6500, and HGVD databases, with a minor allele frequency of ≥ 0.001. In addition, mapping errors were removed by visual inspection using the Integrative Genomics Viewer browser (https://software.broadinstitute.org/software/igv/).

Analysis of copy number alterations identified by WES

The genomic copy number in the samples examined by WES was analyzed using the signal data calculated from the sequence reads. The copy number alterations were evaluated using an in-house CNACS pipeline (https://github.com/papaemmelab/toil_cnacs). Depth was calculated from the weighted sum of the fragments accounting for length and GC biases during sequencing library amplification. The depths were compared with those of the pooled controls. The genomic copy number was estimated from the depth ratios using the circular binary segmentation method. The allele frequencies of the heterozygous SNPs assessed allelic imbalance covered by >50 reads.

Co-occurrence and mutual exclusivity analyses of genetic alterations

A Poisson–Binomial distribution-based analysis implemented in the R package Rediscover v0.2.0 was performed to identify co-occurring or mutually exclusive pairs of

genetic alterations.

Pathway enrichment analysis

Pathway enrichment analysis of both ranked gene lists was performed using GSEA software (version 4.0.3; https://www.gsea-msigdb.org/gsea/index.jsp) and the R package clusterProfiler v.4.6.2. Gene set enrichment analysis (GSEA) was performed on normalized counts (FPKM). The analysis used the h.all.v.7.4.symbols.gmt (Hallmark) and c5.all.v.7.4.symbols.gmt (Gene Ontology) gene set databases. To identify B cell developmental pathways associated with BCP-ALL, gene set variation analysis[3] was performed on genes differentially upregulated in normal B progenitor cells[4] and relative pathway activity at the level of individual samples was determined using the R package GSVA v1.46.0.

Integrative miRNA-mRNA expression analysis

Integrated analyses of the miRNA and mRNA expression profiles were carried out using the differentially expressed miRNAs and mRNAs. Correlations between miRNA and mRNA expression were identified using the miRComb package v0.9.6. Spearman's correlation coefficients between a given miRNA and its predicted target mRNA were calculated and matched by target prediction using two databases (TargetScan and miRDB). Since miRNAs function as negative regulators, miRNA-mRNA pairs that correlated negatively (adjusted $P < 0.05$), and appeared in at least one of the two databases, were selected.

Splicing analysis

The MAJIQ tool (version 2.3) was used to detect local splice variations (LSVs).[5] MAJIQ was run on the Ensembl-based GFF annotations, disallowing *de novo* calls. Changes in the relative inclusion of LSVs (delta percent inclusion index, dPSI) of at

least 20% at the 95% CI between two given conditions were selected for further analysis. For comparative analysis of splicing with that of the normal B progenitor, the pro-B fraction was used as a control, as described previously.[6]

Cell lines and culture

Human REH cell lines were cultured at 37°C/5% CO_2 in RPMI 1640 medium supplemented with 10% fetal calf serum and 1% penicillin/streptomycin.

Western blotting

Protein samples were separated by SDS-PAGE, transferred to a polyvinylidene difluoride membrane, and probed with specific primary antibodies, followed by horseradish peroxidase (HRP)-conjugated secondary antibodies. Specific bands were visualized by enhanced chemiluminescence using the Clarity Western ECL Substrate (Bio-Rad) and quantified by the ChemiDoc XRS1 System and Image Laboratory software (Bio-Rad). Mouse monoclonal anti-DICER1 (F-10, 1:1,000; Santa Cruz Biotechnology) and mouse polyclonal anti-GAPDH (1:4,000; FUJIFILM Wako) were used as primary antibodies for western blotting. HRP-conjugated anti-mouse IgG Abs (1:4,000; Jackson ImmunoResearch Laboratories) were used as secondary antibodies.

Transduction of REH cell lines with doxycycline-inducible short hairpin RNA

Specific shRNAs targeting human *DICER1* and non-targeting control shRNA (for Luc), were designed and subcloned into the pENTR4-H1tetOx1 and CS-RfA-ETV vectors (RIKEN BRC). The following target sequences were used: *DICER1*-shRNA, 5′-ATTGGCTTCCTCCTGGTTA-3′; Luc-shRNA, 5′-CGTACGCGGAATACTTCGA-3′. For the production of lentivirus, HEK293T cells were transfected with lentiviral vectors by polyethylenimine (Sigma-Aldrich). Forty-eight hours after transfection, viral supernatants were harvested and immediately used for infection, followed by sorting of

successfully transduced cells with FACS Aria III (BD Biosciences). For tetracycline-inducible shRNA expression, doxycycline was added to the cultures at a final concentration of 3 μM for 72h. Knockdown efficiency was determined by western blotting.

Measurement of cell viability

Cells were plated in a normal growth medium in a 96-well cell culture plate (50000 cells per well). Different concentrations of cytarabine (FUJIFILM Wako) were added to the culture medium, and cell viability (%) relative to that of control wells containing cell culture medium and an equivalent amount of vehicle was measured at 48 h in a water-soluble tetrazolium 8 (WST-8) assay using the Cell Counting Kit-8 (Dojin). Absorbance was measured using an iMark Microplate Absorbance Reader (Bio-Rad).

Statistical analysis

Statistical analyses were performed using R (v3.5.0, v3.6.3, and v4.1.0). All *P* values were calculated by two-sided analysis, unless otherwise specified. Student t-test, a paired t-test, Fisher's exact test, the Wilcoxon rank-sum test, and the Wilcoxon signed-rank test were used for group comparisons, and comparisons among multiple groups were analyzed by the Kruskal-Wallis test. Multiple testing was corrected using the Benjamini–Hochberg method. A *P*-value of <0.05 was considered statistically significant.

References

1. Ng SWK, Mitchell A, Kennedy JA, Chen WC, McLeod J, Ibrahimova N, et al. A 17-gene stemness score for rapid determination of risk in acute leukaemia. *Nature 2016 540:7633*. 2016;540(7633):433–437.
2. Stanulla M, Dagdan E, Zaliova M, Möricke A, Palmi C, Cazzaniga G, et al. IKZF1 plus defines a new minimal residual disease-dependent very-poor prognostic

profile in pediatric b-cell precursor acute lymphoblastic leukemia. *Journal of Clinical Oncology*. 2018;36(12):1240–1249.

3. Hänzelmann S, Castelo R, Guinney J. GSVA: gene set variation analysis for microarray and RNA-Seq data. *BMC Bioinformatics*. 2013;14(1):7.
4. Chen D, Zheng J, Gerasimcik N, Lagerstedt K, Sjögren H, Abrahamsson J, et al. The expression pattern of the Pre-B cell receptor components correlates with cellular stage and clinical outcome in acute lymphoblastic leukemia. *PLoS One*. 2016;11(9):e0162638.
5. Norton SS, Vaquero-Garcia J, Lahens NF, Grant GR, Barash Y. Outlier detection for improved differential splicing quantification from RNA-Seq experiments with replicates. *Bioinformatics*. 2018;34(9):1488–1497.
6. Black KL, Naqvi AS, Asnani M, Hayer KE, Yang SY, Gillespie E, et al. Aberrant splicing in B-cell acute lymphoblastic leukemia. *Nucleic Acids Res*. 2018;46(21):11357–11369.

Supplementary Figure 1.

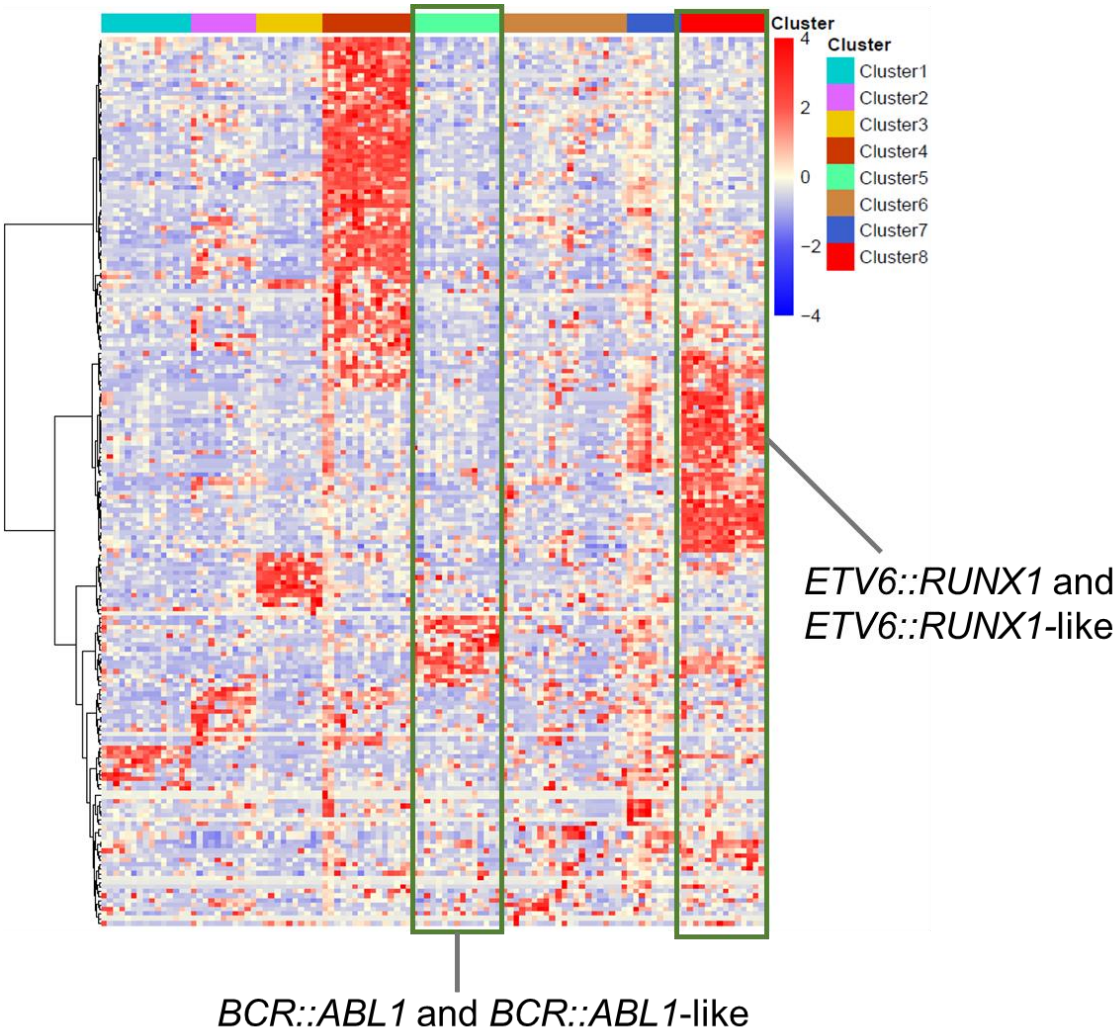

Gene expression clusters in the 111 BCP-ALL samples from the TARGET cohort. The ROSE method identified 198 genes, including the top 25 genes in clusters 1-8 of the TARGET cohort. Ward's hierarchical clustering method was used for clustering analysis of the ROSE gene set. Four samples had a *BCR::ABL1*-like signature with no known fusion genes, and three samples had an *ETV6::RUNX1*-like signature.

Supplementary Figure 2.

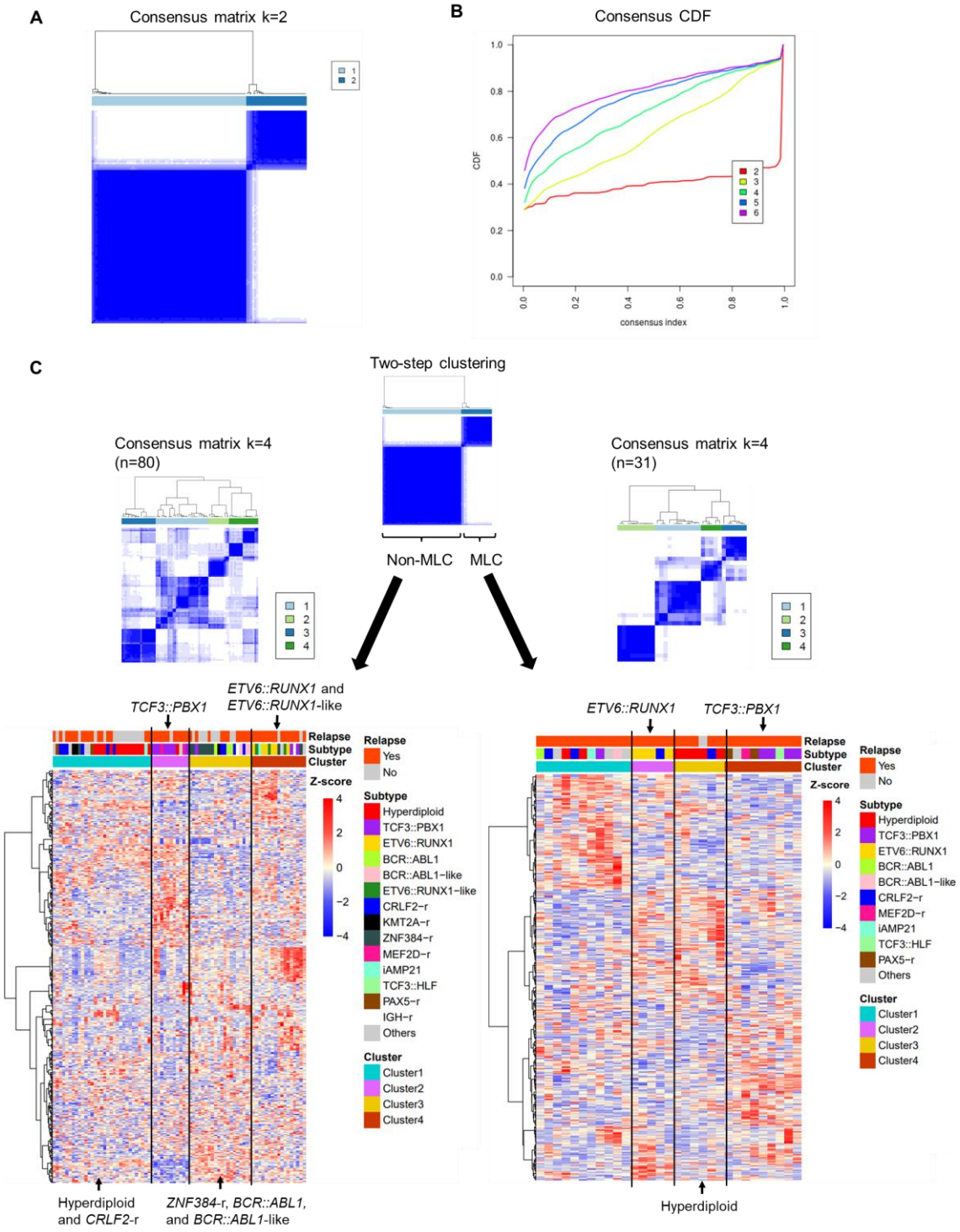

Consensus clustering analysis of miRNA expression in 111 BCP-ALL cases.

(A) Consensus matrix and (B) CDF plots showing consensus clustering of all 111 samples. (C) Two-step unsupervised consensus clustering restricted to the non-MLC

cases (n = 80) and MLC cases (n = 31) respectively. Consensus matrix and miRNA expression heatmap generated using 500 probes across 80 non-MLC primary samples, along with clinical information for each case.

Supplementary Figure 3.

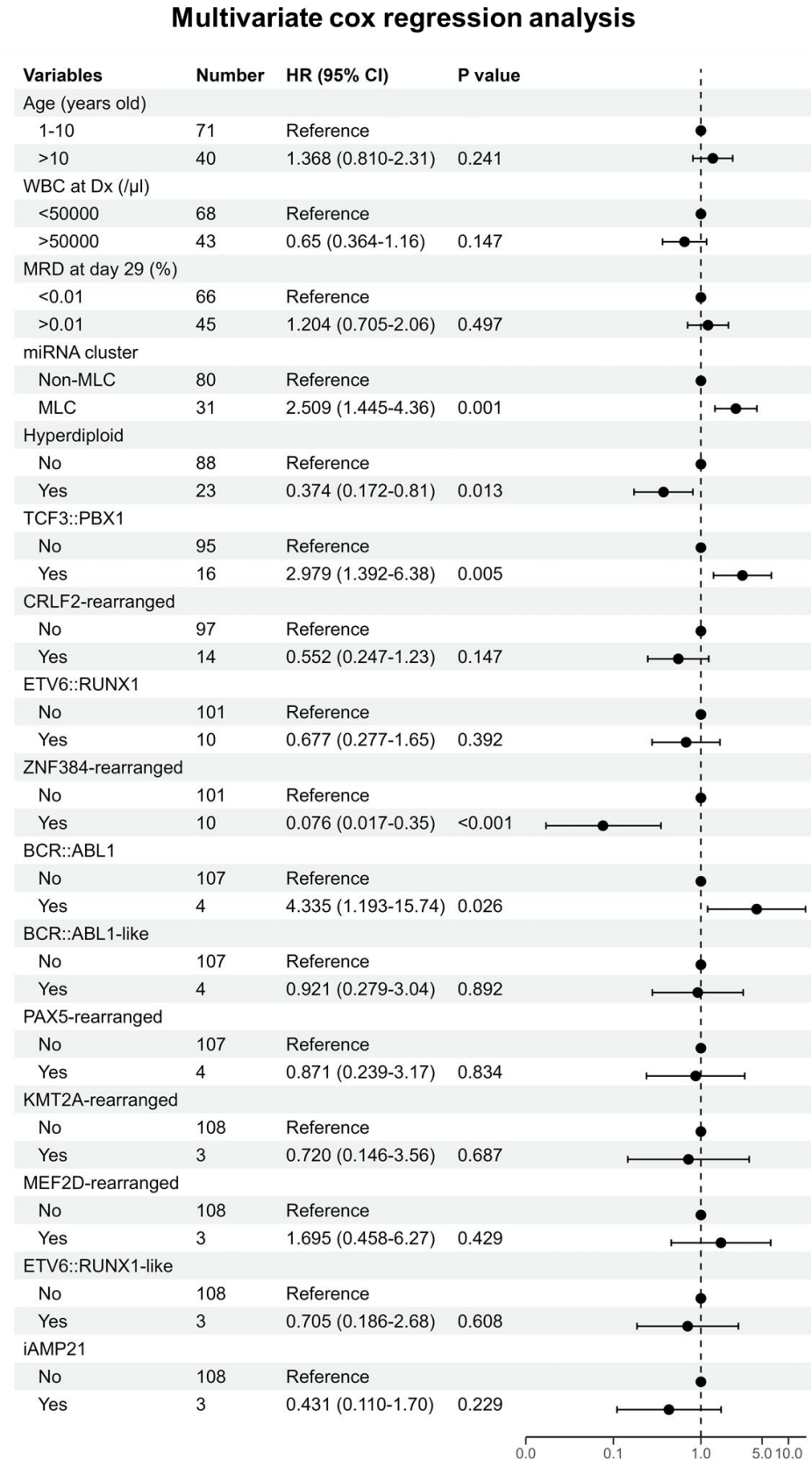

Forest plot showing the results of multivariate Cox regression analysis of the effect of different parameters, including genetic subtype, on event-free survival.
Squares represent the hazard ratio and horizontal lines represent the confidence interval (CI). WBC at Dx, white blood cell count at diagnosis; MRD, minimal residual disease.

Supplementary Figure 4.

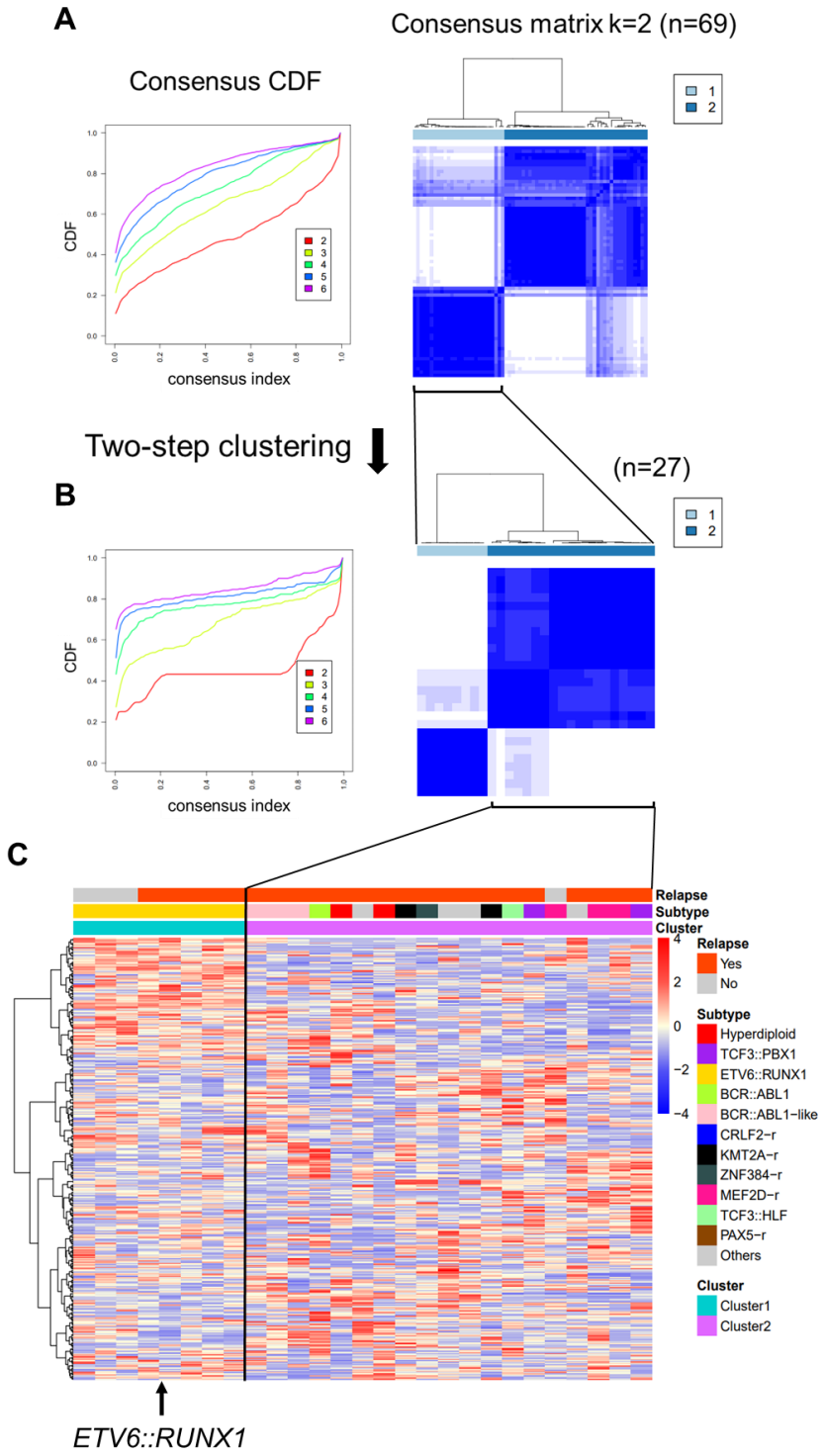

Two-step consecutive unsupervised consensus clustering of miRNA expression by 69 BCP-ALL cases in the Japanese cohort.

(A) CDF plots and consensus matrix showing consensus clustering of the 69 samples. (B) CDF plots and consensus matrix showing consensus clustering of 27 samples confined to the first cluster shown in (A). (C) Heatmap of miRNA expression generated using 400 probes across 27 samples, along with clinical information for each case.

Supplementary Figure 5.

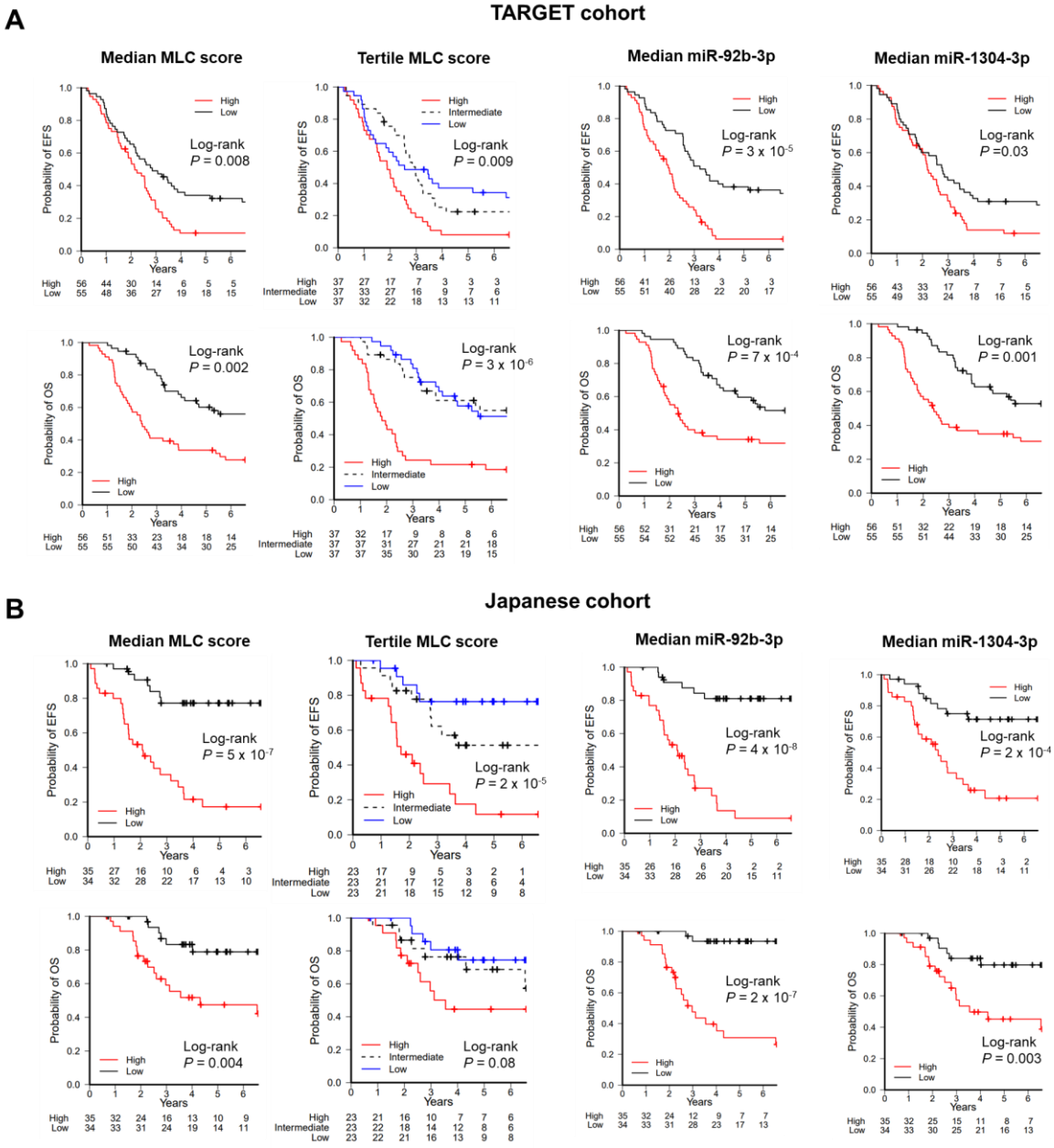

Prognostic value of MLC scores, miR-92b-3p and miR-1304-3p in BCP-ALL cases. Kaplan–Meier survival curves of event-free survival (EFS) and overall survival (OS) for BCP-ALL cases with high or low level of the MLC score, miR-92b-3p and miR-1304-3p in the TARGET cohort (A) and the Japanese cohort (B). The cut-off for stratification was set to median or tertile for the MLC score and median for miRNAs. P values are based on the log-rank test.

Supplementary Figure 6.

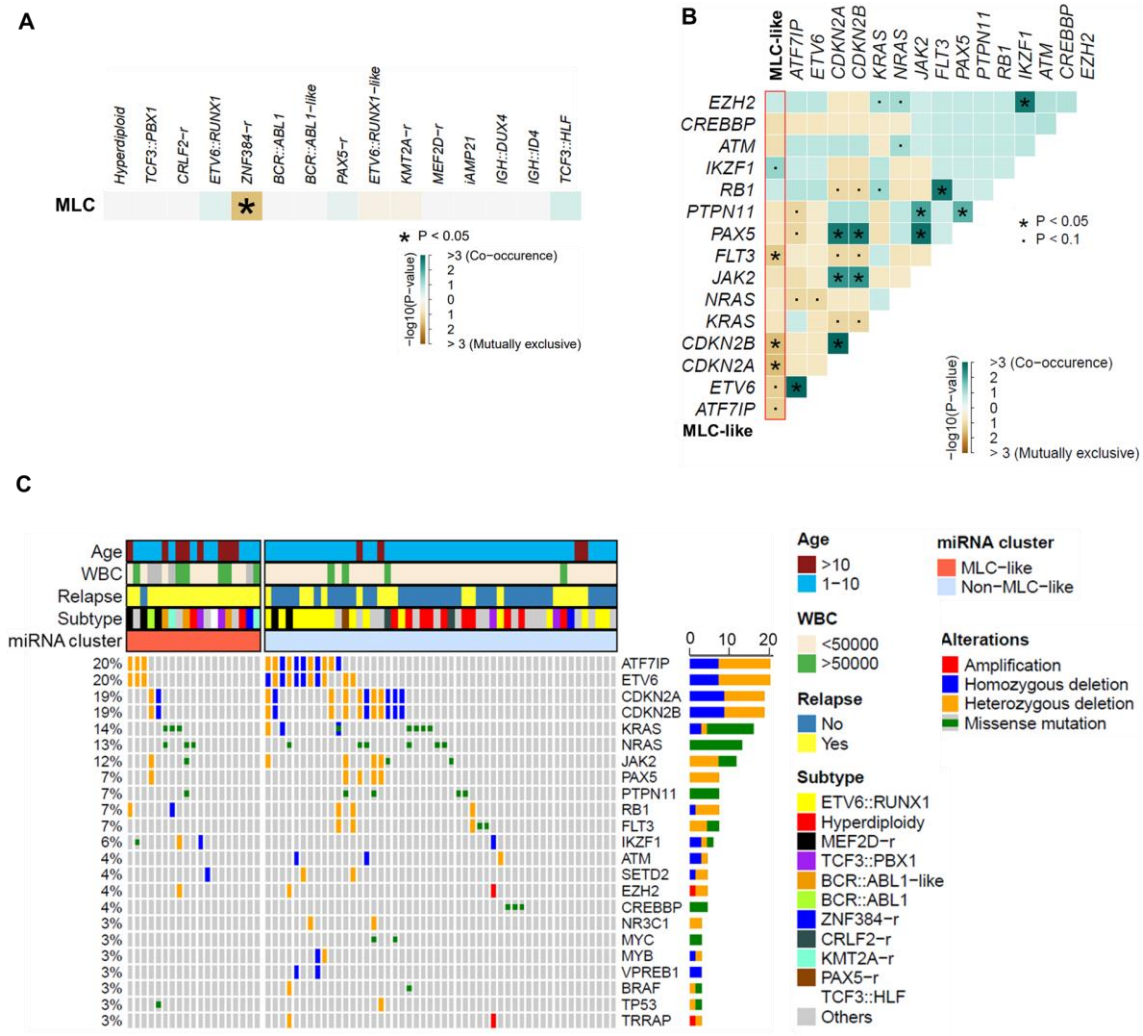

Gene mutations in MLC and MLC-like BCP-ALL cases.

Co-occurrence or mutual exclusivity between genetic subtype and MLC signature pairs in 111 BCP-ALL primary samples from the TARGET cohort (A), and co-occurrence or mutual exclusivity between gene mutations and MLC-like signature pairs in 69 BCP-ALL primary samples from the Japanese cohort (B). Green indicates a tendency toward co-occurrence, and brown indicates exclusivity. The point indicates $P < 0.1$, and the asterisk indicates $P < 0.05$. (C) Recurrent driver mutations and copy number alterations identified by WES, based on clinical information for the 69 BCP-ALL primary samples from the Japanese cohort. Cases are grouped as MLC-like and non-MLC-like according to miRNA expression cluster. WBC, white blood cell count.

Supplementary Figure 7.

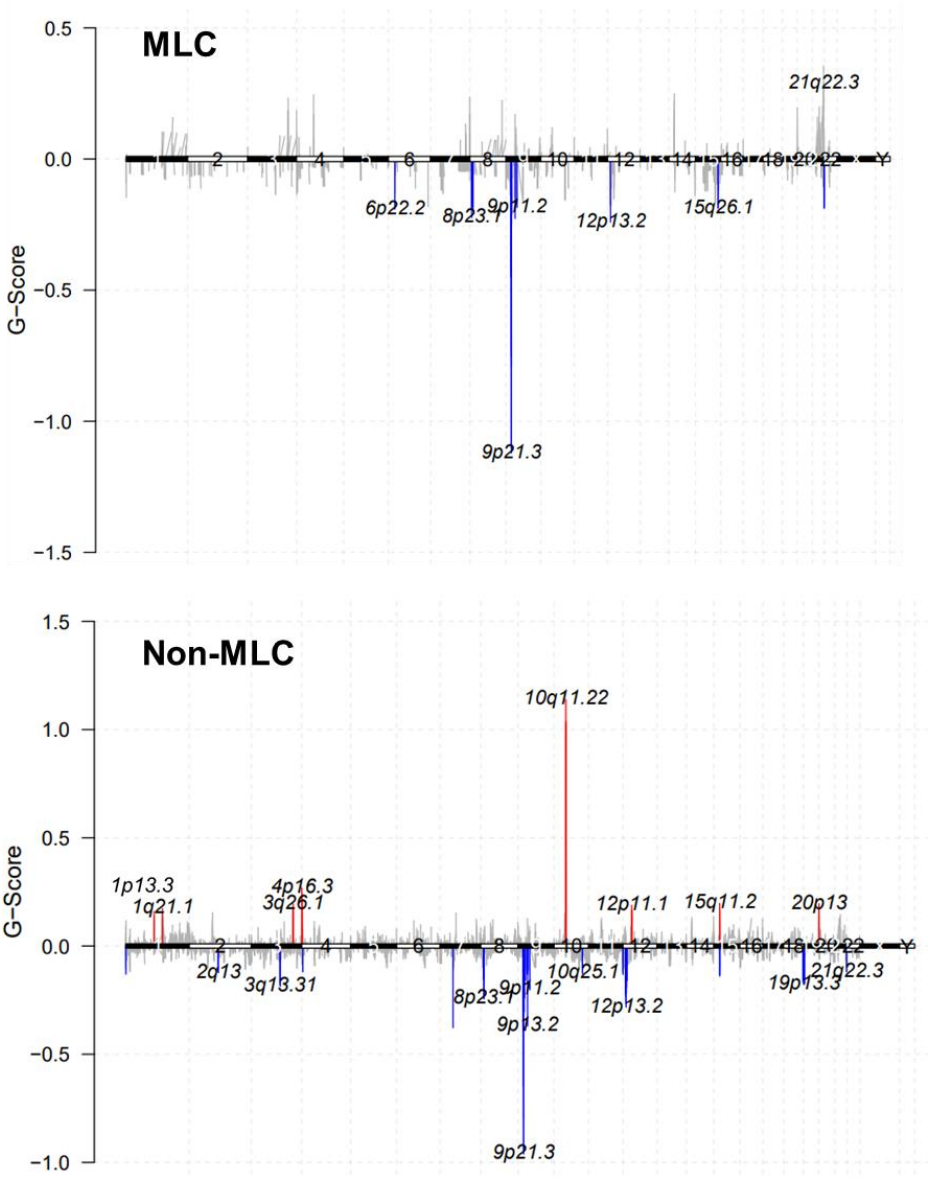

Copy number alterations in MLC and non-MLC of BCP-ALL cases.
Statistically significant copy number gains and losses detected by the GISTIC algorithm are shown for 105 BCP-ALL primary samples (31 MLC and 74 non-MLC) from TARGET cohort SNP array data. MLC in the top panel; non-MLC in the bottom panel.

Supplementary Figure 8.

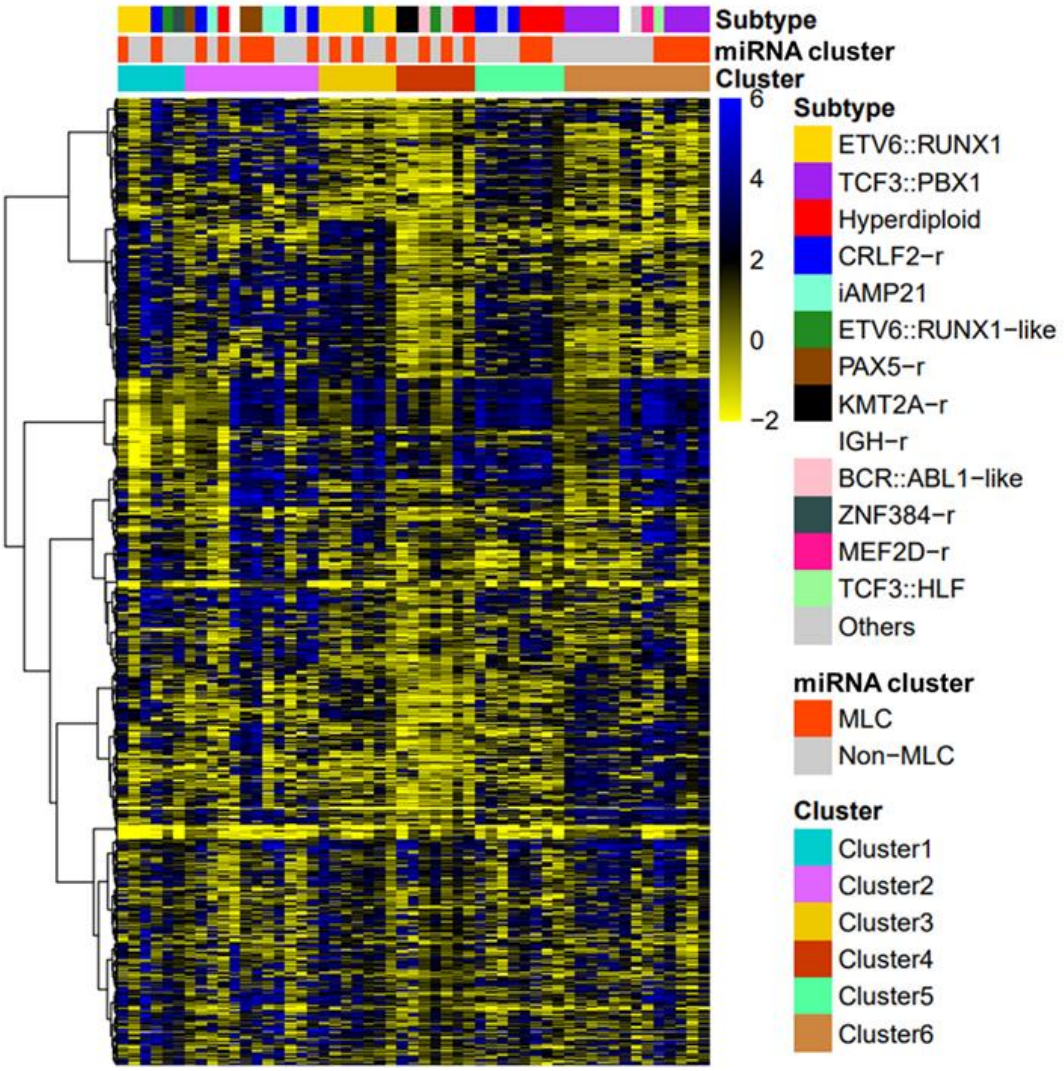

Hierarchical clustering of DNA methylation profiles for the MLC and non-MLC BCP-ALL cases.

The heatmap shows the DNA methylation profiles of 53 BCP-ALL cases (22 MLC and 31 non-MLC) based on unsupervised hierarchical clustering using the HpaII to MspI ratio from the HELP Assay along with Roche NimbleGen from the TARGET cohort. Six clusters were identified by consensus clustering with 1000 probes (distance method: Pearson).

Supplementary Figure 9.

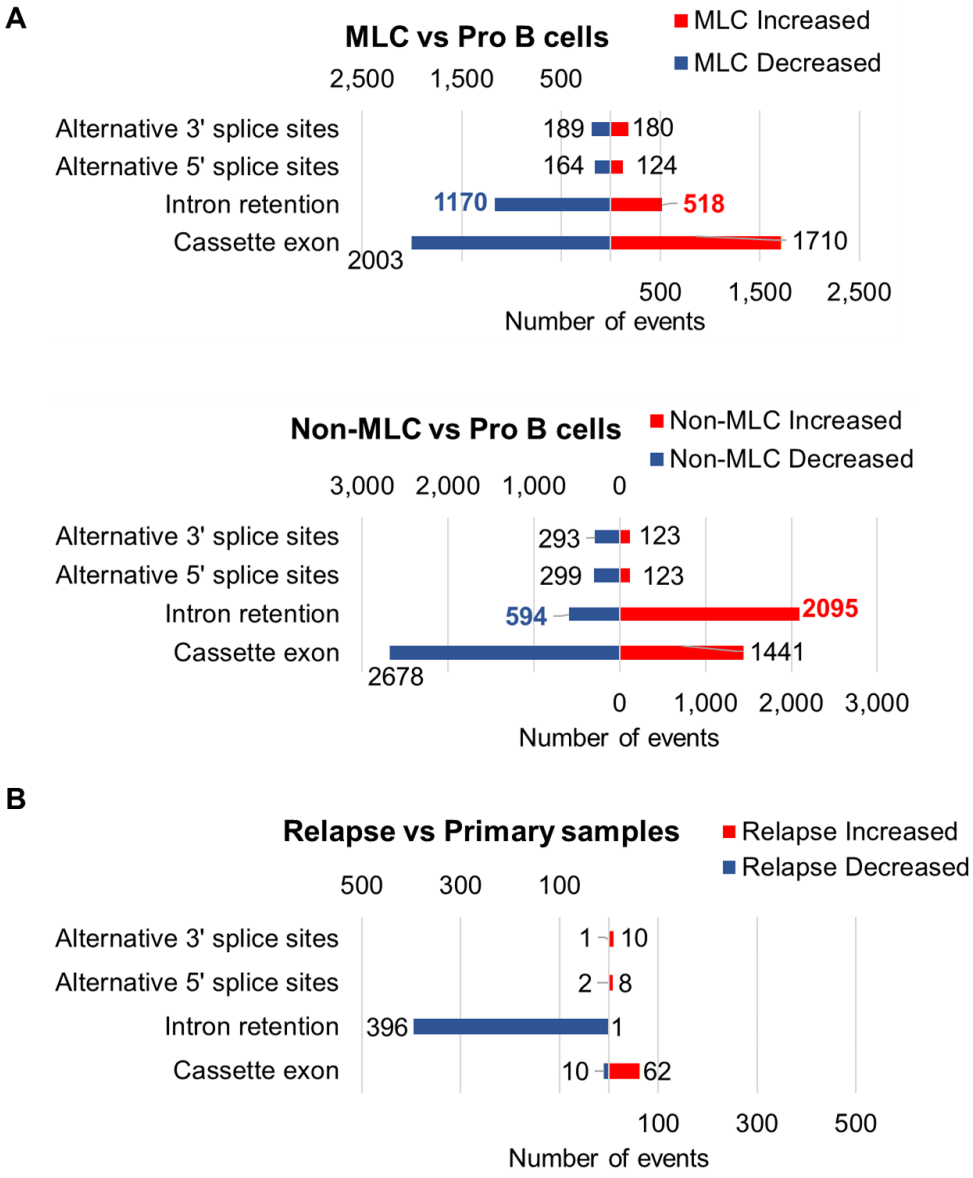

Alternative RNA splicing of MLC and relapsed cases.

(A) Type and number of splicing alterations significantly associated with MLC cases compared with normal pro-B cells (top), and with non-MLC cases compared with normal pro-B cells (bottom). (B) Type and number of splicing alterations significantly associated with relapsed samples compared with paired-primary samples from nine relapsed cases that acquired the MLC-like profile at relapse. Changes in the relative inclusion of local splice variations of at least 20% at the 95% confidence interval between two given conditions are shown. Bars on the right indicate alternative splicing events that were increased, and bars on the left indicate those that were decreased.

Supplementary Figure 10.

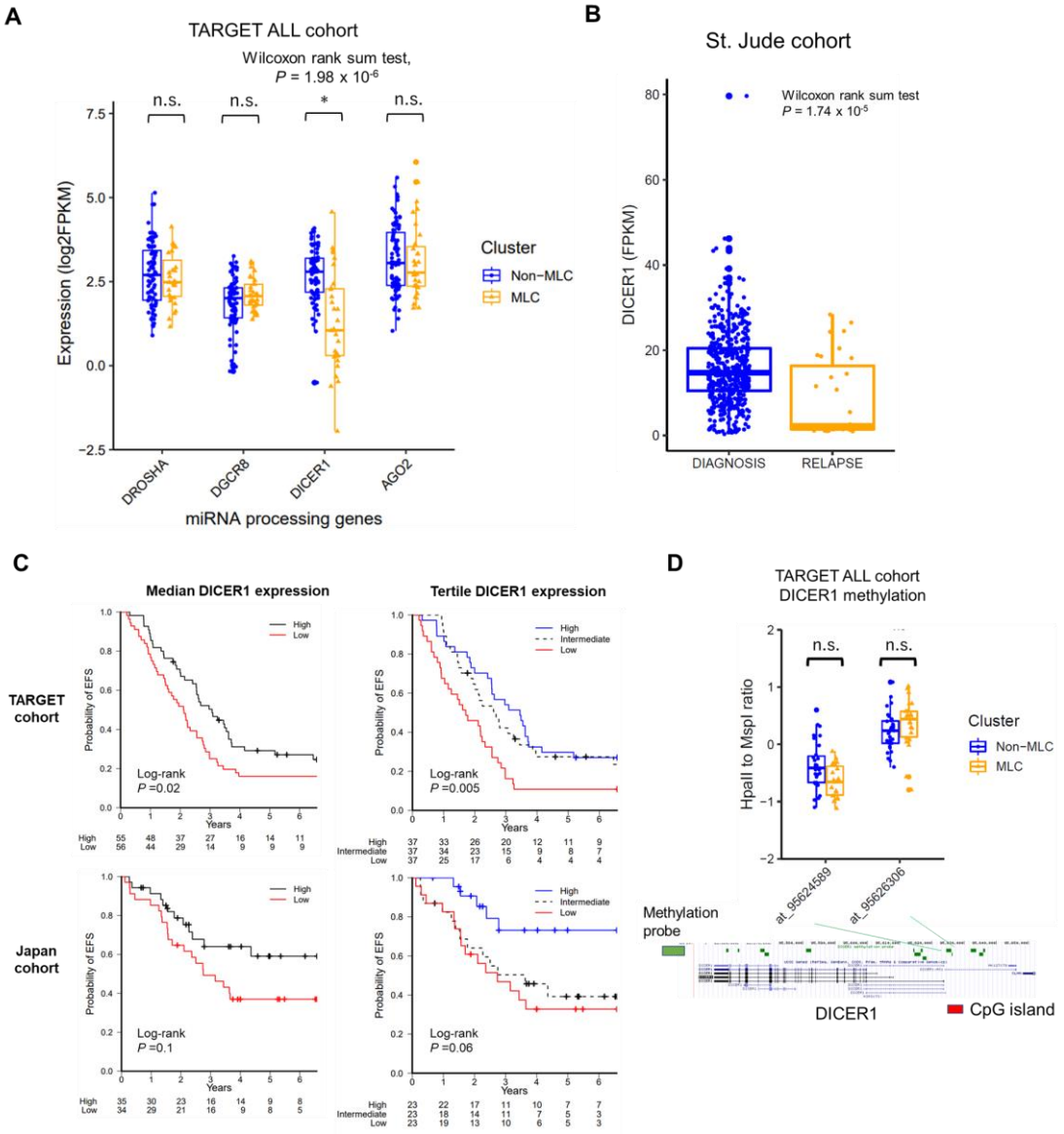

***DICER1* expression and methylation in BCP-ALL.**

(A) Box plots comparing miRNA processing genes (*DROSHA, DGCR8, DICER1* and *AGO2*) expression (expressed as log2 of fragments per kilobase million (FPKM)) by non-MLC cases (n = 80), and MLC cases (n = 31) from the TARGET ALL cohort. The P-value was calculated using the Wilcoxon rank-sum test. (B) Box plots comparing *DICER1* expression (expressed as FPKM) in primary samples (n = 501) and relapse samples (n = 31) from the B-ALL cohort (n = 532) from the St. Jude Cloud database. The *P* value was calculated using the Wilcoxon rank-sum test. (C) Kaplan–Meier survival curves of event-free survival (EFS) and overall survival (OS) for BCP-ALL

cases with high or low level of the *DICER1* expression in the TARGET ALL and Japanese cohorts. The cut-off for stratification was set to median or tertile for *DICER1* expression. (D) Box plot showing quantification of DNA methylation using the HpaII to MspI ratio from the HELP Assay, along with Roche NimbleGen of the CpG island probe targeting the *DICER1* promoter (at_95624589 and at_95626306) in non-MLC cases (n = 31) and MLC cases (n = 22) from the TARGET ALL cohort. The Wilcoxon rank-sum test was used to evaluate the differences. n.s., not significant.